

Brief Reports

Brief Reports are short papers which report on completed research which, while meeting the usual *Physical Review* standards of scientific quality, does not warrant a regular article. (Addenda to papers previously published in the *Physical Review* by the same authors are included in Brief Reports.) A Brief Report may be no longer than $3\frac{1}{2}$ printed pages and must be accompanied by an abstract. The same publication schedule as for regular articles is followed, and page proofs are sent to authors.

Observation of the effect of refraction on x rays diffracted in a grazing-incidence asymmetric Bragg geometry

Michael F. Toney

IBM Research Division, IBM Almaden Research Center, San Jose, California 95120-6099

Sean Brennan

Stanford Synchrotron Radiation Laboratory, P.O. Box 4349, Stanford, California 94309

(Received 27 July 1988; revised manuscript received 21 November 1988)

The positions of x-ray diffraction peaks from a polycrystalline iron oxide thin film have been measured in a grazing-incidence, asymmetric Bragg geometry for incidence angles between 0.09° and 1.04° . The peak positions are shifted from the Bragg angles $2\theta_B$ due to refraction of the incident x rays as they penetrate the air-solid interface. The shifts are quantitatively consistent with those obtained by applying Fresnel boundary conditions for reflection and refraction of a plane electromagnetic wave at an interface between air and a uniform, absorbing dielectric and they provide confidence in the validity of the Fresnel boundary conditions in the x-ray regime.

X rays traveling through matter are weakly scattered in the forward direction with the scattered wave undergoing a $-\pi/2$ phase shift.¹⁻³ This forward-scattered wave interferes with the incident wave and builds up a wave that travels through the material with a phase velocity that is slightly larger than the speed of light, c . Thus, the index of refraction at x-ray energies is slightly less than 1, which leads to refraction when x rays are incident onto an interface between two different materials. One manifestation of refraction is total external reflection when the incidence angle is less than the critical angle for total external reflection. Another is a change in direction of x rays as they penetrate the interface between two substances. Since the forward scattering, and hence the deviation of the refractive index from 1, are quite small, refractive effects are largest at very small incidence angles. In this paper we report the observation of these effects by measuring shifts in diffracted peak positions from an iron oxide thin film as the grazing-incidence angle is varied near the critical angle.

Figure 1 shows the grazing-incidence, asymmetric Bragg (GIAB) geometry used in these experiments.^{4,5} The x rays are incident on the solid at a small angle ϕ and are reflected at the same angle ϕ . The refracted x rays travel in the solid with an angle ϕ' , are diffracted through the Bragg scattering angle $2\theta_B$, and are then refracted again as they exit the solid. As shown below, this later refraction, and the change in refraction as ϕ varies, is very small, since $2\theta_B$ is large, and will be neglected. The measured scattering angle is 2θ , which is different from $2\theta_B$.

In most theoretical treatments of the situation in Fig. 1 (including the one given below),^{1,6} the problem is approx-

imated as a boundary-value problem for reflection and refraction of a plane electromagnetic wave at an interface between air and a uniform, absorbing dielectric. This results in the classic Fresnel equations.⁷ Although there is a great deal of experimental evidence from x-ray reflectivity measurements that this is a valid approximation,^{8,9} it is not immediately obvious, since at x-ray energies the wavelength of light is comparable to atomic dimensions (e.g., the width of the interface).

In this usual approximation,^{1-3,6} the effects of refraction at x-ray energies are taken into account by treating the solid as a uniform dielectric with an index of refraction given by

$$n = 1 - \delta - i\beta, \quad (1)$$

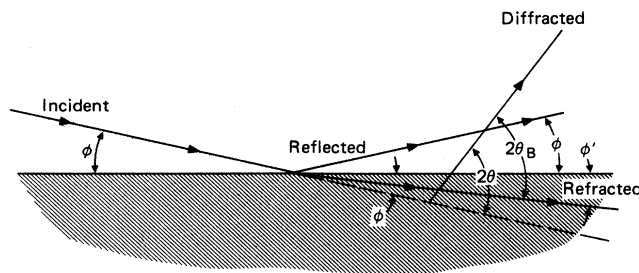


FIG. 1. Schematic representation of GIAB diffraction geometry in the vertical plane of the diffractometer. The angles of incidence and reflection are ϕ , the refracted angle is ϕ' , the Bragg scattering angle is $2\theta_B$, and the measured scattering angle is 2θ . The dashed line continues along the direction of the incident x rays. The x and z directions are parallel and perpendicular to the surface, respectively.

where

$$\delta = \frac{e^2}{2\pi mc^2} N_0 \frac{\rho(Z+f')}{A} \lambda^2 = 2.70 \times 10^{-6} \frac{Z+f'}{A} \rho \lambda^2 \quad (2)$$

and

$$\beta = \lambda \frac{\mu}{4\pi}.$$

Here N_0 is Avogadro's number; Z , the average atomic number; A , the average atomic mass; ρ , the mass density; f' , the average of the real part of the anomalous scattering factor; μ , the linear absorption coefficient; and λ , the x-ray wavelength. For x rays incident from air (δ and β essentially zero) onto a solid (or liquid) surface, Snell's law is $\cos\phi = n \cos\phi'$. Since δ and β are quite small ($\sim 10^{-6}$) and ϕ and ϕ' are also small, this reduces to

$$\phi' = [(\phi^2 - \phi_c^2) - 2i\beta]^{1/2}, \quad (3)$$

where $\phi_c = \sqrt{2\delta}$ is the critical angle for total external reflection and is typically several tenths of a degree.

Inside the solid the electric field vector is $\mathcal{E}(0)e^{-ik'_z r}$, where $\mathcal{E}(0)$ is the field at the surface and

$$\mathbf{k}' = kn(\cos\phi', \sin\phi') = k(\cos\phi, \sin\phi') \approx k(1, \phi'). \quad (4)$$

Since the z component of \mathbf{k}' is complex (ϕ' is complex), it is convenient to break \mathbf{k}' into real and imaginary parts, $\mathbf{k}' = \mathbf{k}'_r - ik'_z \hat{z}$, where \hat{z} is the unit vector in the z direction (into the solid). Thus, the electric field in the solid is

$$\mathcal{E}(0)\exp[-i[(k'_r)_x x + (k'_r)_z z]] \exp(-k'_z z), \quad (5)$$

where $(k'_r)_x$ and $(k'_r)_z$ are, respectively, the x and z components of \mathbf{k}'_r . From this it is seen that the direction of the refracted x rays in the solid is

$$\begin{aligned} \frac{(k'_r)_z}{(k'_r)_x} &= \text{Re} \left[\frac{(n \sin\phi')}{\cos\phi} \right] \\ &\approx \text{Re}(\phi') \\ &= \frac{1}{\sqrt{2}} \{[(\phi^2 - \phi_c^2)^2 + 4\beta^2]^{1/2} - \phi_c^2 + \phi^2\}^{1/2}, \quad (6) \end{aligned}$$

where Re refers to the real part thereof.

For planes in the polycrystalline sample that are aligned to diffract the x rays traveling through the sample, the measured scattering angle 2θ will be different from the Bragg angle $2\theta_B$. By referring to Fig. 1, it can be seen that 2θ will be shifted from $2\theta_B$ by

$$\begin{aligned} 2\Delta\theta &= 2\theta - 2\theta_B \\ &= \phi - \frac{(k'_r)_z}{(k'_r)_x} \\ &\approx \phi - \frac{1}{\sqrt{2}} \{[(\phi^2 - \phi_c^2)^2 + 4\beta^2]^{1/2} - \phi_c^2 + \phi^2\}^{1/2}. \quad (7) \end{aligned}$$

The magnitude of this shift in 2θ can be estimated by noting that the maximum shift occurs near ϕ_c and is $2\Delta\theta = \phi_c - \sqrt{2}\beta$, while at zero and very large incidence angles the shift is essentially zero. Thus, the peak shifts

should be of the order of several tenths of a degree, which is readily observable.

Since β is much smaller than δ , absorption is only important very close to ϕ_c (within about 0.02°). Away from this region and for $\phi < \phi_c$, Eq. (7) reduces to $2\Delta\theta = \phi$. This linear dependence is easily understood. Below the critical angle the x rays are evanescent within the sample and travel exactly parallel to the surface (neglecting absorption). Thus, the diffracted x rays make a constant angle $2\theta_B$ with respect to the surface and 2θ varies linearly with incidence angle. For $\phi \gg \phi_c$, Eq. (7) can be approximated as $\phi_c^2/(2\phi)$, which is small for large ϕ . This approximation is not valid for large ϕ , since a small-angle approximation was used to derive Eq. (7). However, it is easy to show that when the small-angle approximation does not hold, Eq. (7) is accurately approximated by $(\phi_c^2/2)(1 + \sin^2\phi)(\sin\phi \cos\phi)^{-1}$. From this it is seen that in the GIAB geometry, refraction of the diffracted x rays as they exit the solid (see Fig. 1) can be ignored. For the values of $2\theta_B$ in our experiment, the exiting x rays are refracted less than 0.003° . More important, as ϕ varies in the range of our experiments, the extent of refraction will change, causing 2θ to shift. Since we are measuring the change in 2θ as ϕ varies, it is more significant that this change is extremely small ($< 0.0003^\circ$).

The $\gamma\text{-Fe}_2\text{O}_3$ thin-film sample was prepared^{10,11} by reactive sputtering of a 0.75 at. % Os-doped Fe target in an Ar-O₂ plasma and subsequent oxidation in air at 300°C for 2 h. In work to be reported elsewhere,¹¹ we show that this sample is heterogeneous with a surface layer of $\alpha\text{-Fe}_2\text{O}_3$, while the bulk of the film is predominantly $\gamma\text{-Fe}_2\text{O}_3$. The substrates were very flat, polished Si(100) single crystals. The high degree of flatness ensured that the grazing incidence angle was constant across the sample. The experiments were performed using the GIAB geometry as shown schematically in Fig. 1 and described in detail elsewhere.^{4,5,12} Data were taken at the eight-pole focused wiggler station 7-2 of the Stanford Synchrotron Radiation Laboratory (SSRL) and a Si(111) double-crystal monochromator was used to select an incident x ray of 6800 eV (wavelength of 1.823 Å). The incident beam was defined with 1-mm vertical and horizontal slits so the entire sample was illuminated for all incidence angles. The scattered beam was collimated with 0.06° (1 mrad) Soller slits and collected with a scintillation counter.

Data were taken for values of ϕ from 0.085° to 1.035° by scanning the detector from $2\theta = 29^\circ$ ($Q = 1.73 \text{ \AA}^{-1}$) to $2\theta = 46^\circ$ ($Q = 2.69 \text{ \AA}^{-1}$). At $\phi = 0.0^\circ$, the sample is exactly parallel to the incident x rays; however, it is difficult to accurately achieve this alignment experimentally. In these experiments, the alignment of ϕ to zero was done roughly and a small (constant) offset is needed to convert the experimental ϕ into absolute ϕ (where $\phi = 0$ corresponds to the sample parallel to the incident beam). In work to be reported elsewhere,¹¹ this offset is determined from measurements of the intensities of the $\alpha\text{-Fe}_2\text{O}_3$ and $\gamma\text{-Fe}_2\text{O}_3$ diffraction peaks as a function of ϕ . This offset is $+0.034 \pm 0.004^\circ$. All ϕ values reported here have this adjustment taken into account.

Figure 2 shows the $\gamma\text{-Fe}_2\text{O}_3$ (213) diffraction peak for

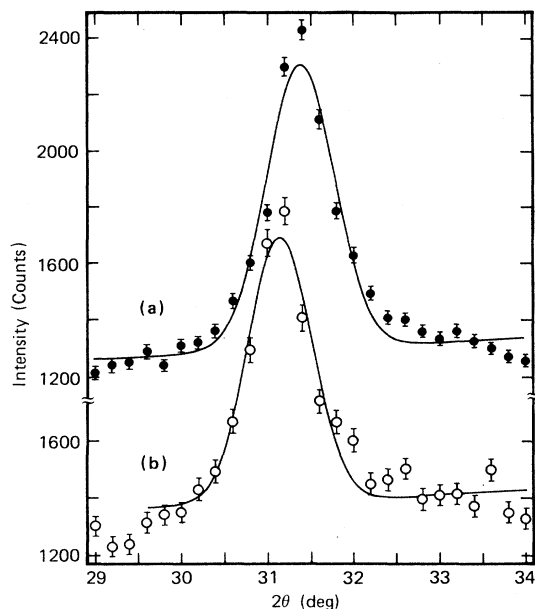


FIG. 2. Polycrystalline diffraction patterns from the iron oxide thin film at two different incidence angles showing the γ - Fe_2O_3 (213) diffraction peak. The lines are least-squares fits to the data using a Gaussian line shape and a linear background. (a) $\phi = 0.375^\circ$, (b) $\phi = 1.035^\circ$. The peak shift is clearly evident.

two grazing incidence angles. Figure 2(a) is for $\phi = 0.375^\circ$, which is very close to the critical angle ($\phi_c = 0.365^\circ$), while Fig. 2(b) is for $\phi = 1.035^\circ$, which is much larger than the critical angle. The lines are least-squares fits to the data with a Gaussian line shape and a linear background.¹¹ These data show that the position of the γ - Fe_2O_3 (213) diffraction peak has shifted from $2\theta = 31.4^\circ$ at $\phi = 0.375^\circ$ to $2\theta = 31.1^\circ$ at $\phi = 1.035^\circ$. This 0.3° shift is caused by the refraction of the incident x rays described above and its magnitude is consistent with that estimated from Eq. (7).

As the incidence angle decreases below ϕ_c , the x-ray penetration depth and the x-ray intensity at the surface decrease rapidly.^{5,6} As mentioned above, the iron oxide sample is heterogeneous and has a surface layer of α - Fe_2O_3 , which is significantly thicker than the x-ray penetration depth for $\phi < \phi_c$.¹¹ The decrease in penetration depth and in surface x-ray intensity are large enough that the x-ray intensity in the γ - Fe_2O_3 phase becomes very small as ϕ decreases below ϕ_c . Thus, the intensity of the γ - Fe_2O_3 (213) peak is also very small and we are not able to accurately measure the position of this diffraction peak for incidence angles less than 0.3° . However, there are several other diffraction peaks in the measured range of 2θ . These include the γ - Fe_2O_3 (300) and γ - Fe_2O_3 (313) for γ - Fe_2O_3 and the α - Fe_2O_3 (104) and α - Fe_2O_3 (110) for α - Fe_2O_3 . Figure 3(a) shows the shifts $2\Delta\theta$ for these peaks and the γ - Fe_2O_3 (213) as a function of ϕ . To determine $2\Delta\theta$, it is necessary to know or determine $2\theta_B$. Since thin films often have large strains, it is not possible to use the bulk d spacings to calculate $2\theta_B$. Thus, for each of the five reflections, $2\theta_B$ is determined from a

least-squares fit of Eq. (7) to the measured 2θ as a function of ϕ . This value of $2\theta_B$ is then subtracted from the data and the resulting $2\Delta\theta$ is plotted in Fig. 3(a). The solid line is the shift calculated from Eq. (7). We note that since the density of α - and γ - Fe_2O_3 are essentially the same, refraction at the α - Fe_2O_3 / γ - Fe_2O_3 interface is extremely small.

Due to the number of data points in Fig. 3(a), the experimental errors in $2\Delta\theta$ are not shown. Instead, the weighted averages of $2\Delta\theta$ for all the observed diffraction peaks and their associated errors are shown in Fig. 3(b). Again, the solid line is the shift calculated from Eq. (7). The agreement between theory and experiment is excellent and Fig. 3 clearly shows the directional change in x

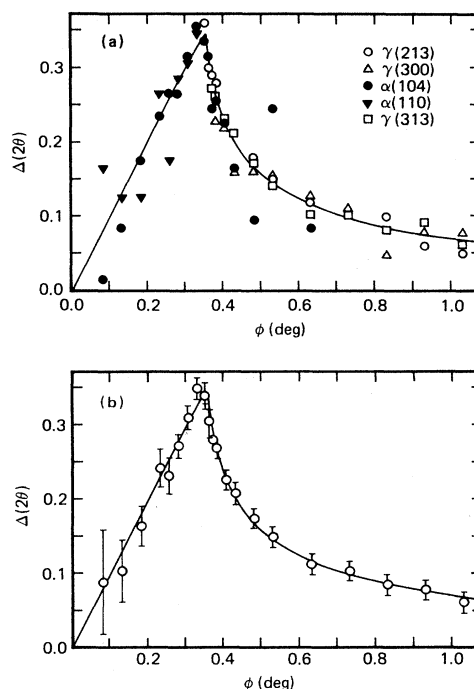


FIG. 3. Shift in scattering angle, $2\Delta\theta = 2\theta - 2\theta_B$. The solid line is calculated from Eq. (7) for iron oxide ($\rho = 5.2 \text{ g/cm}^3$, $f' = -1.8$, $\mu = 253.7 \text{ cm}^{-1}$) at 6800 eV incident x-ray energy. (a) Data for γ - Fe_2O_3 (213), γ - Fe_2O_3 (300), α - Fe_2O_3 (104), α - Fe_2O_3 (110), and γ - Fe_2O_3 (313). Note that the peaks from the α - Fe_2O_3 phase are mostly observed for $\phi < \phi_c$, while those from γ - Fe_2O_3 are observed for $\phi > \phi_c$. This occurs because, as ϕ decreases below ϕ_c , the x-ray penetration depth becomes sufficiently smaller than the thickness of the α - Fe_2O_3 surface layer and the surface x-ray intensity decreases enough that the x-ray intensity in the γ - Fe_2O_3 phase of the sample is very small (Refs. 5 and 12). The values of $2\theta_B$ subtracted from 2θ to obtain $2\Delta\theta$ are γ - Fe_2O_3 (300), $2\theta_B = 38.34^\circ$ ($d = 2.777 \text{ \AA}$); α - Fe_2O_3 (104), $2\theta_B = 39.25^\circ$ ($d = 2.714 \text{ \AA}$); γ - Fe_2O_3 (313), $2\theta_B = 42.47^\circ$ ($d = 2.517 \text{ \AA}$); α - Fe_2O_3 (110), $2\theta_B = 42.29^\circ$ ($d = 2.527 \text{ \AA}$); and γ - Fe_2O_3 (213), $2\theta_B = 31.10^\circ$ ($d = 3.401 \text{ \AA}$). For γ - Fe_2O_3 the d spacings are quite close to those expected from bulk (Ref. 13), while for α - Fe_2O_3 the spacings are about 0.5% larger, presumably due to strain. (b) Weighted average of $2\Delta\theta$ using data from (a). A value of $\chi^2 = 0.67$ demonstrates the excellent agreement between the theory and experiment.

rays that is caused by refraction. This indicates that the use of the classical Fresnel boundary conditions is valid even at x-ray energies, where the wavelength is comparable to atomic dimensions. The use of Fresnel boundary conditions appears valid because the Ewald-Oseen extinction theorem, which is generally only valid in the dipole or low-frequency limit (when the light wavelength is large compared with the dimensions of the scatterers), is also applicable when the incident radiation frequency is high compared to atomic transition frequencies, which is true for x-ray radiation.¹⁴

James has derived an expression for $2\Delta\theta$ under conditions where dynamical effects are important but total external reflection and absorption are unimportant.¹ In a grazing incidence geometry, his expression is well approximated by $\delta/(\sin\phi) \sim \phi_c^2/(2\phi)$, the same as the expression given earlier for $\phi \gg \phi_c$. However, for ϕ close to ϕ_c , the effects of total external reflection become very important and James's expression is a poor approximation to the correct expression [Eq. (7)]. This may explain previous differences¹² between observed shifts $2\Delta\theta$ and those calculated using $\phi_c^2/(2\phi)$. It also demonstrates the necessity of using Eq. (7) rather than the approximation by James when accurate lattice constants of thin films are measured using a highly asymmetric Bragg geometry. Since experiments have recently been conducted using a grazing-exit (take-off) angle,¹⁵ we note that the effects de-

scribed above will also exist in this geometry.

To summarize, we have observed the directional change in x rays resulting from refraction by measuring the diffraction peak shifts $2\Delta\theta$ from a polycrystalline iron oxide thin film. The data are in excellent quantitative agreement with a calculation of the peak shifts obtained by treating the sample as a uniform dielectric with index of refraction $n = 1 - \delta - i\beta$ and applying the Fresnel boundary conditions for reflection and refraction of a plane electromagnetic wave at an interface. This result provides confidence in the validity of the Fresnel boundary conditions at x-ray energies, despite the fact that x-ray wavelengths are comparable to interfacial widths. The adequacy of this classical approach is apparently due to the validity of the Ewald-Oseen extinction theorem in the x-ray regime.¹⁴ These data also demonstrate the importance of accounting for refraction in accurate measurements of lattice constants in thin films using an asymmetric Bragg geometry.

The work described here was partially done at SSRL. Partial funding for this research has been provided by the U.S. Department of Energy under Contract No. DE-AC03-82ER13000 (Division of Chemical Sciences and Division of Materials Sciences of the Office of Basic Energy Sciences). We thank Mao Min Chen and Gil Castillo for preparing the iron oxide sample.

¹R. W. James, *The Optical Principles of the Diffraction of X-rays* (Ox Bow, Woodbridge, 1982).

²C. G. Darwin, *Philos. Mag.* **27**, 315 (1914); **27**, 675 (1914).

³A. H. Compton, *Philos. Mag.* **45**, 1121 (1923).

⁴T. C. Huang, M. F. Toney, S. Brennan, and Z. Rek, *Thin Solid Films* **154**, 439 (1987).

⁵M. F. Toney, T. C. Huang, S. Brennan, and Z. Rek, *J. Mater. Res.* **3**, 351 (1988).

⁶G. H. Vineyard, *Phys. Rev. B* **26**, 4146 (1982).

⁷M. Born and E. Wolf, *Principles of Optics* (Pergamon, Oxford, 1980).

⁸A. H. Compton and S. K. Allison, *X-rays in Theory and Experiment* (Van Nostrand, Princeton, 1935).

⁹A. H. Compton, *Bull. Nat. Res. Council. (U.S.)* **20**, 48 (1922).

¹⁰M. M. Chen, C. Ortiz, G. Lim, R. Sigsbee, and G. Castillo, *IEEE Trans. Magn.* **MAG-23**, 3424 (1987).

¹¹M. F. Toney and S. Brennan, *J. Appl. Phys.* (to be published).

¹²G. Lim, W. Parrish, C. Ortiz, M. Bellotto, and M. Hart, *J. Mater. Res.* **2**, 471 (1987).

¹³Powder Diffraction File, Joint Committee on Powder Diffraction Standards, International Center for Diffraction Data, Swarthmore, PA, 1986. Card No. 13-534 for α -Fe₂O₃ and No. 25-1402 for γ -Fe₂O₃.

¹⁴D. W. Oxtoby, F. Novak, and S. A. Rice, *J. Chem. Phys.* **76**, 5278 (1982).

¹⁵D. P. Osterman, K. Mohanty, and J. D. Axe, *J. Phys. C* **21**, 2635 (1988).